NRIAG Journal of Astronomy and Geophysics (2016) 5, 306–312

National Research Institute of Astronomy and Geophysics

NRIAG Journal of Astronomy and Geophysics

www.elsevier.com/locate/nrjag

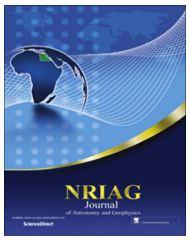

Assessment of the wastewater effect on the shallow subsurface soil at Farafra Oasis, Egypt, by using geoelectrical and geochemical data analysis

Mahmoud Ismail Ismail Mohamaden

National Institute of Oceanography and Fisheries, Kayet Bey, El Anfoushy, Alexandria, Egypt

Received 13 February 2016; revised 30 May 2016; accepted 31 May 2016
Available online 16 June 2016

KEYWORDS

Farafra Oasis;
Groundwater;
V.E.S.;
Aquifer

Abstract Geoelectrical techniques have been used to detect the subsurface stratigraphy and structures around Farafra Oasis, Egypt. 1D inversion approaches have been applied to interpret the geoelectrical data obtained at six vertical electrical soundings (VES's) using the well-known Schlumberger array with half-current electrode spacing (AB/2) varying from 3 to 400 m in successive steps.

A preliminary quantitative interpretation of the sounding curves was achieved firstly by using two-layer standard curves and generalized Cagniard graphs. The final models were obtained in 1D using IPI2WIN program. The modeling results were used to construct two geoelectrical sections.

Two geoelectrical units were identified: the superficial geoelectrical layer is composed mainly of shale (Dakhla Shale Formation). It is characterized by relatively very low electrical resistivity values (3–5 Ω m) with a maximum thickness of about 17.58 m.

The second layer reveals moderate electrical resistivity values (17–98 Ω m). It is extended from the surface layer to the end of the investigated section and represents the Sandstone (upper aquifer) in the study area.

1. Introduction

Farafra Oasis (Fig. 1) is one of the oases in the New Valley Governorate that economically depends on agricultural activities which release a large amount of the agricultural drainage water. Such water is collected through drainage canals in the vacant and uncultivated lands forming wastewater pond. The wastewater pond exists at a highland area. So, there is a risk of collapsing of the pond's wall and flooding of the wastewater to the neighboring cultivated lands.

E-mail address: Mahmoud_Moha12@Yahoo.com

Peer review under responsibility of National Research Institute of Astronomy and Geophysics.

ELSEVIER Production and hosting by Elsevier

http://dx.doi.org/10.1016/j.nrjag.2016.05.003

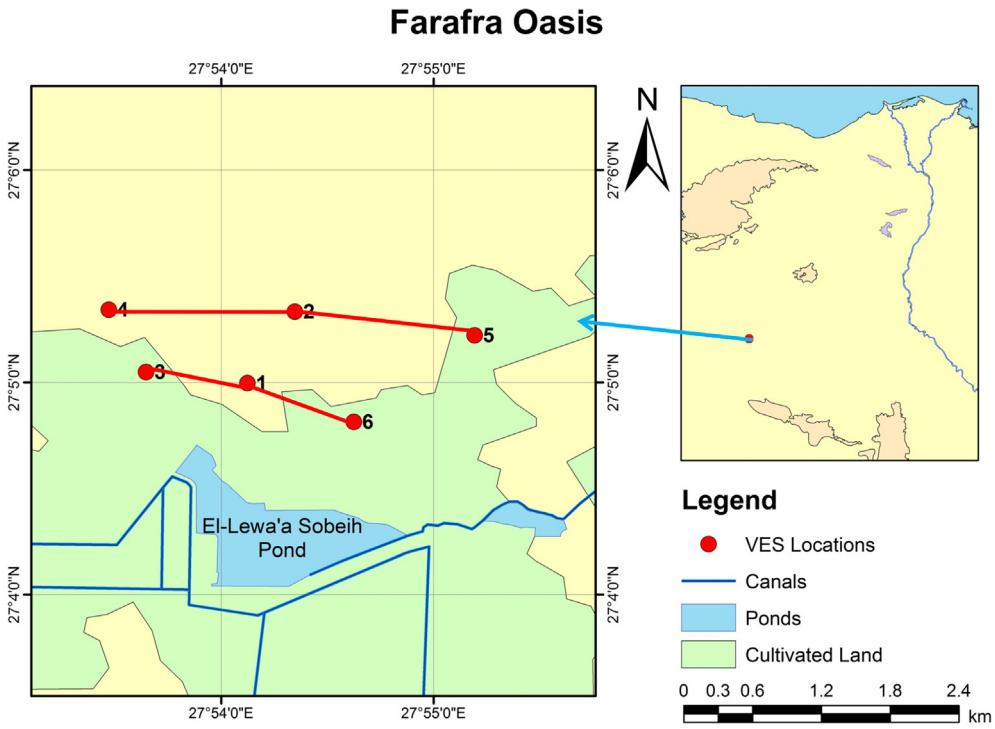

Figure 1 Location map for Farafra Oasis showing VES locations.

The wastewater flood may contaminate the shallow subsurface soil. Also, the leakage of water into the underground aquifer represents serious threats for the population in this region, and especially they are totally dependent on groundwater. The presence of an impermeable layer such as shale and clays prevents the leakage of the wastewater into the underground fresh water aquifer.

The main objectives of this study were as follows:

- Identification of the shallow subsurface layers in this area.
- Determination of the shale distribution and the possibility of leakage through the different areas around the ponds and determination of the suitable areas for further agricultural activities using the wastewater.
- Examination of the probable soil contamination due to the wastewater effect.

Geophysical investigation is a powerful tool for exploring the subsurface geology and collecting more information about the subsurface layers and structures (Mohamaden et al., 2009; El-Sayed, 2010). In this study, geoelectrical resistivity method was used for shallow subsurface investigation to determine the distribution and thickness of the shale layer.

Besides, some soil samples have been chemically analyzed to investigate the possibility of soil contamination. The total heavy metal concentrations were determined according to Oregioni and Aston (1984). Heavy metals were measured by using flame-atomic absorption spectrophotometer. The grain size analysis was applied according to Folk (1980). The carbonate content was determined by Molnia (1974). The total organic carbon (TOC) content was determined using Gaudette Loring and Rantala, 1992. The total phosphorus (TP) content was determined according to Aspila et al. (1976) and Murphy and Riley (1962).

1.1. Geology of Farafra Oasis

Farafra Oasis is located at 140 km southwest of the Bahariya Oasis in the central part of the Western Desert (between 26°45′, 27°40′N and 27°00′, 28°50′E) as shown in Fig. 2. Similar to Bahariya Oasis, Farafra Oasis occupies an oval-shaped depression with an area of ~10,000 km^2. On the bottom of Farafra depression, the Dakhla Shale (Maastrichtian) is outcropped, and it is extended laterally into the Maastrichtian Khoman Chalk in the central and northern parts of the oasis (Hermina, 1990; Issawi et al., 2009). Farafra depression is surrounded by high escarpments, and its bottom rises gradually to the general level of the surrounding desert southward (Beadnell, 1901; Said, 1962; Issawi et al., 2009). The scarps of Farafra depression are composed of the Tarawan Formation (Paleocene) overlain by Esna Shale (Paleocene–lower Eocene) and Farafra Limestone (lower Eocene) (Issawi et al., 2009; Orabi and Zaky, 2016). The eastern part of the depression is covered by sand sheets, and the depression is bounded to the west by the Great Sand Sea (Fig. 2). Farafra depression forms a dome structure, which represents the southern extension of the Syrian Arc System (Omara et al., 1970). Its axis stretches in the NE–SW direction.

2. Methodology

2.1. Geoelectrical data

Many authors such as Koefoed (1965a,b,c), Gosh (1971), Zohdy (1975,1989), Santos et al. (2006), Sultan and Santo (2008a,b and 2009a,b,c,d), Sultan et al. (2009), Mohamaden (2001, 2005 and 2008), Mohamaden and Abu Shagar (2008), Abbas and Sultan (2008), and Mohamaden et al. (2009).

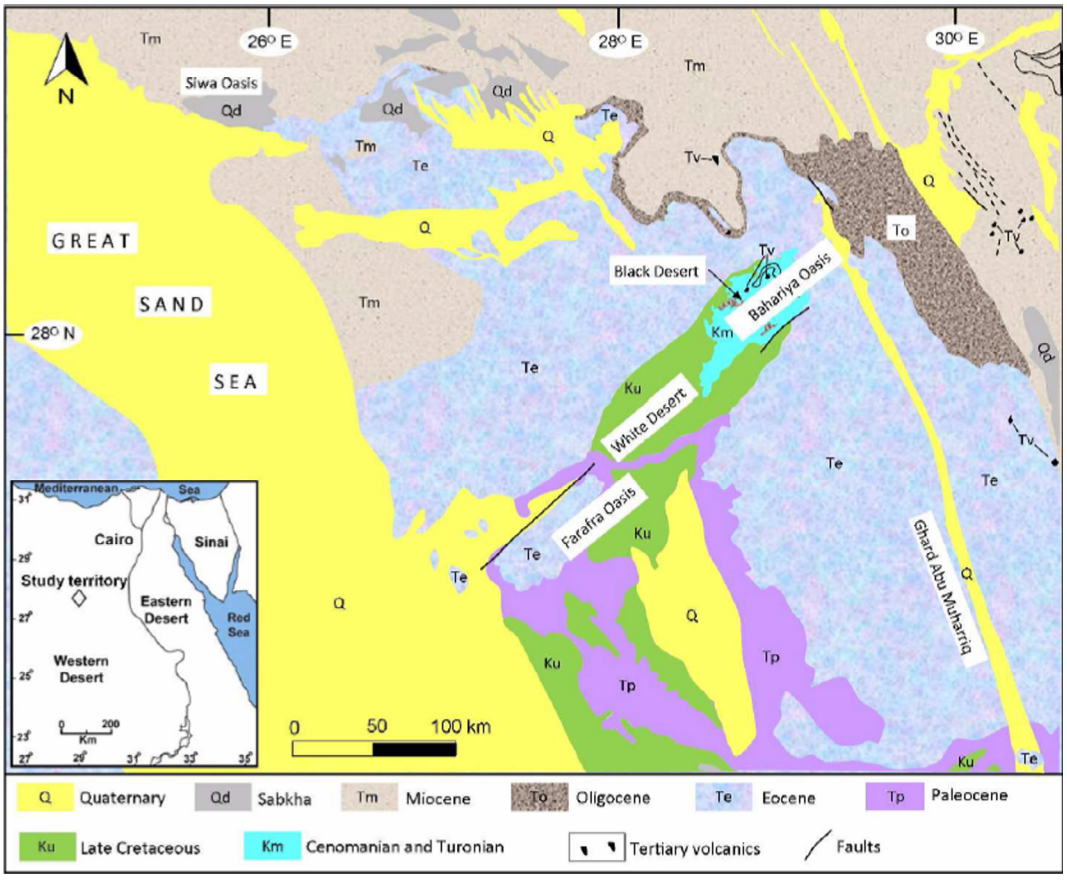

Figure 2 Geologic map of Farafra Oasis.

Hemeker (1984) studied the quantitative interpretation of the geoelectrical resistivity measurements.

The electrical resistivity survey consists of a transmitter, receiver, power supply, stainless steel electrodes, and shielded cables. In the present study, IRIS SYSCAL-PRO instrument is used which computes and displays apparent resistivity for many electrode configurations. The geoelectrical configuration used in the study is Schlumberger collinear four symmetrical electrode configurations. The current electrode separation was varying from 3 to 400 m in successive steps.

The result of the geoelectrical survey was processed and quantitatively interpreted using available geologic information and presented as geoelectrical sections along the various profiles.

The obtained data are plotted using ready-made software in order to be processed and interpreted. After data processing and interpretation, layer parameters (true resistivities and thicknesses or depths) of the various current penetrated layers can be obtained (El-Sayed, 2010).

At this study, the area under investigation was covered by 6 vertical electrical soundings along two profiles named profiles 1 and 2 (Fig. 1). These profiles run from east to west.

The interpretation of the apparent electrical resistivity data was achieved using two methods; the first is based on curve matching technique using Generalized Cagniard Graph method constructed by Koefoed (1965a,b,c), and the output results are treated according to the inverse problem method using computer program (IPI2win). Then results were represented as geoelectrical section.

The Pseudo-Section for apparent electrical resistivity (qualitative interpretation) and the geoelectrical resistivity sections obtained from the quantitative interpretation of vertical electrical soundings revealed the following.

2.1.1. Profile 1

The Pseudo-Section for apparent electrical resistivity as a tool for qualitative interpretation of the vertical electrical sounding data shows that (Fig. 3): the area at the extremely west of this profile is characterized by low apparent electrical resistivity values referred that this area is covered by Dakhla Shale Formation.

The Geoelectrical Section for this profile (quantitative interpretation) deduced that (Fig. 4).

The superficial geoelectrical layer is formed from shale. It is characterized by low electrical resistivity values (3–5 Ω m) and depth ranges from 2.56 to 6.96 m. It covers the ground surface at the extremely two ends of this profile.

At the maximum depth of penetration, we can detect the second geoelectrical layer. It formed from Sandstone with moderate electrical resistivity (17–36 Ω m) corresponding to sandstone layer saturated with wastewater seeped from the oxidation pond at the area under investigation.

The most promising area, for land reclamation and agriculture activities, occupies the two ends of this profile where the shale (Dakhla Shale) layer attains a maximum thickness.

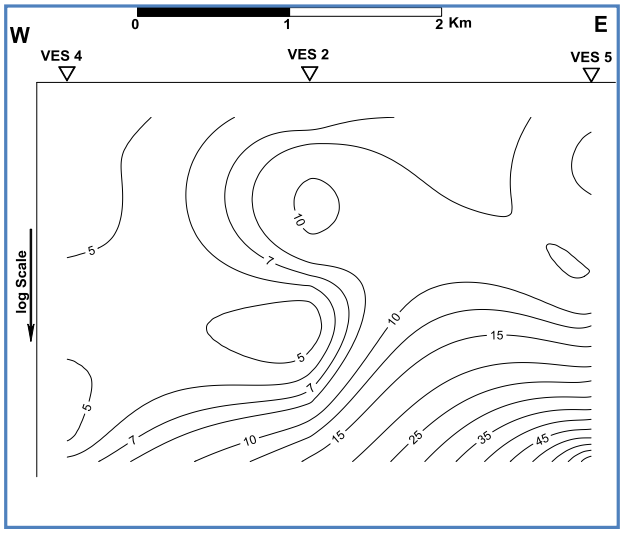

Figure 3 Pseudo-Section for apparent electrical resistivity for profile 1.

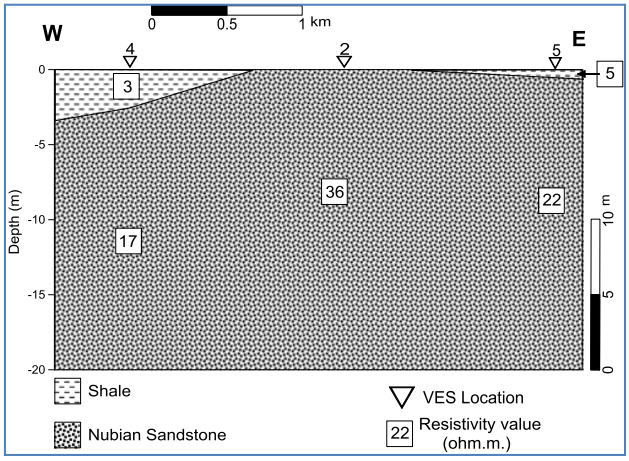

Figure 4 Geoelectrical section for profile 1.

2.1.2. Profile 2

The Pseudo-Section for apparent electrical resistivity as a tool for qualitative interpretation of the vertical electrical sounding data shows that (Fig. 5).

This profile is covered by thickness of Dakhla Shale Formation as the result of relatively low apparent electrical resistivity values.

The Geoelectrical Section for this profile (quantitative interpretation) deduced that (Fig. 6).

The superficial geoelectrical layer is formed from shale. It is characterized by low electrical resistivity values (3–4 Ω m) and depth ranges from 10.56 to 17.58 m. It covered the ground surface along this profile. The second geoelectrical layer represents the saturated Sandstone layer from the seepage of the wastewater with moderate electrical resistivity (18–98 Ω m). It is the upper most aquifer at the area under investigation.

This profile is the most promising area for land reclamation where the Dakhla Shale Formation is represented with large thickness.

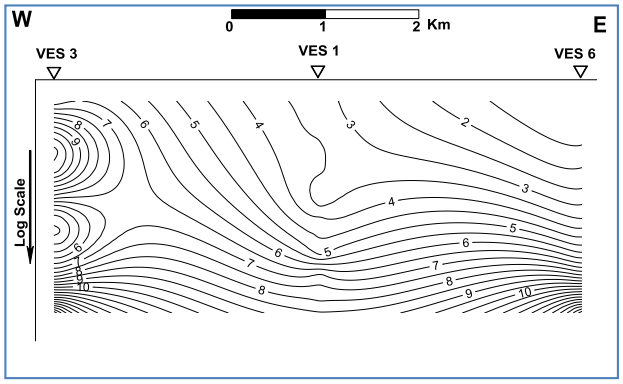

Figure 5 Pseudo-Section for apparent electrical resistivity for profile 2.

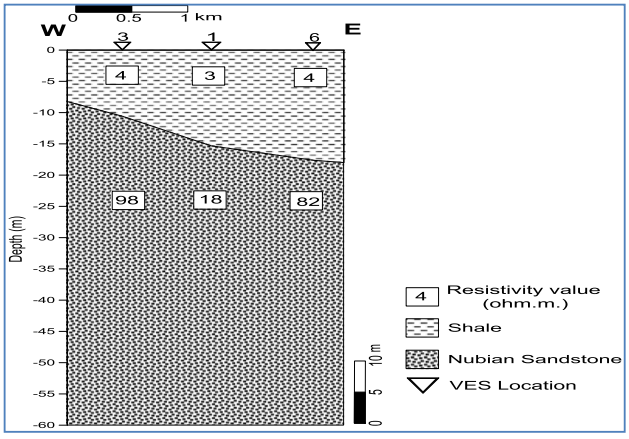

Figure 6 Geoelectrical section for profile 2.

2.2. Geochemical analysis

Six soil samples were collected from Farafra Oasis land. The samples were collected from the same locations at which the VES data were measured. Five sediment samples are in the **sand** range between coarse and medium sand (VES1: VES5) with 94.85–99.56% sand and 0.44–5.15% **mud**, and one sample (VES6) is fine sand with 16.07% sand and 83.93% mud. In general, the mud % and mean % decrease toward the northern direction away from El-Lewa'a Sobeih pond with inversely trend with sand% which increases toward the northern direction (Fig. 7).

Low level (0.06–0.13%) of total organic carbon (TOC) was determined in the soil samples, with exception of VES 5 which shows a TOC level of 0.47%. The total carbonate content ranges from 33.23% to 56.4% in the samples except for VES 5 which is 78.12%.

The total phosphorus content ranges between maximum value 197 μg/g and 749 μg/g with an average value of 376 μg/g. The average value is lower than the average P concentration of 700 μg/g for standard shale (Turekian and Wedepohl, 1961). Comparatively, the range of total phosphorus in the Egyptian top soil of Nile origin is 650–1780 μg/g with an average is 1200 μg/g (Balba, 1985).

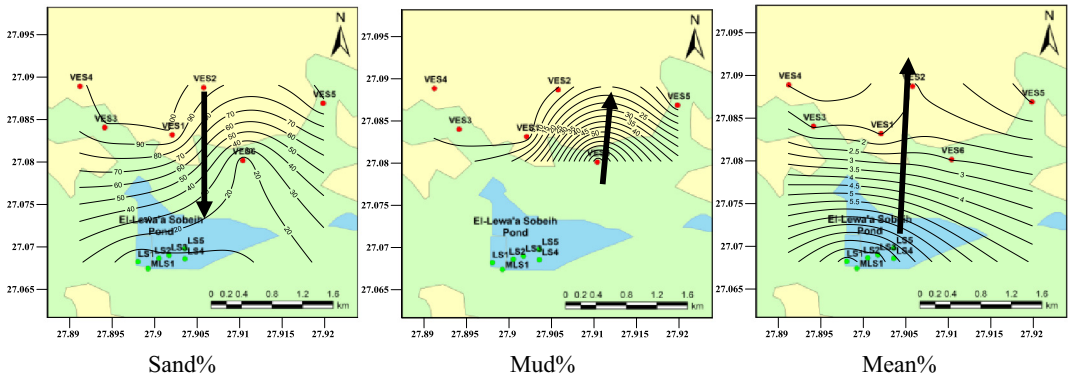

Figure 7 Mechanical analysis for samples.

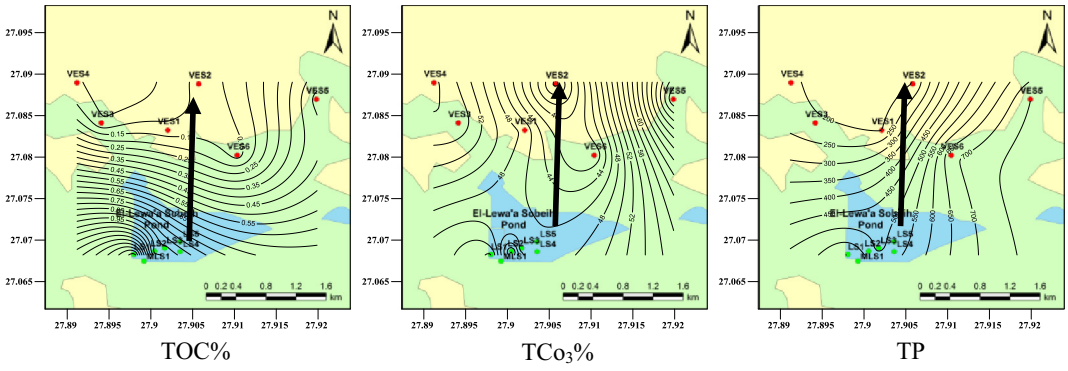

Figure 8 Distribution of TOC%, TCO_3% and TP.

Table 1 Concentrations of heavy metals of the soil (mg/kg).

Station	Lat	Long	Sand	Mud	Mean	TOC	TCO_3	TP	Fe	Zn	Cu	Pb	Cd
			%					μg/g					
VES 1	27.08327	27.90206	99.15	0.85	1.44	0.12	47.53	197	7692	49.12	1.18	28.32	0.07
VES 2	27.08888	27.90578	94.85	5.15	1.55	0.12	33.23	201	8193	25.78	0	33.42	0.53
VES 3	27.08414	27.8941	99.23	0.77	1.41	0.06	55.67	212	1804	28.97	0.56	27.99	0.14
VES 4	27.08903	27.89118	98.31	1.69	0.97	0.06	56.47	211	10,971	29.32	1.96	29.8	0.18
VES 5	27.08702	27.91988	99.56	0.44	0.46	0.47	78.12	749	436	41.25	1.94	18.68	0.44
VES 6	27.08023	27.9104	16.07	83.93	2.45	0.13	40.24	687	13,009	78.1	7.39	35.6	0.88

As shown in Fig. 8, the percentage of total organic carbon, total carbonate percentage and total phosphorous are decreased toward the northern direction.

Total metal content for **Farafra** sediments ranges from 436 μg/g to 13,009 μg/g, 25.78 to 78.10 μg/g, 0.0 to 7.39 μg/g, 18.68 to 35.60 μg/g and 0.07 to 0.88 μg/g for Fe, Zn, Cu, Pb and Cd, respectively as shown in Table 1.

The studied heavy metals have been compared with Quality Standard for Soils (GB 15,618–1995), Canadian soil quality guidelines (CSQG) of Canadian Council of Ministers of the Environment (CCME) (2007) and European Union Standards (EU, 2002) as well as with average upper earth crust of Wedepohl to evaluate pollution (see Table 2).

Comparison of element concentrations in topsoils with Grade I and II criteria for soil quality that were established to protect agricultural production and to maintain human health showed that the determined element concentrations were generally low. Only one sample for Pb exceeded Grade I. Fe concentrations in the study area are lower than the average upper earth crust values for all studied samples. The typical iron concentrations in soils range from 0.2% to 55% (20,000–550,000 mg/kg) (Bodek et al., 1988), and concentrations can vary significantly, even within localized areas, due to soil types and the presence of other sources.

Zn, Pb and Cd concentrations of the study area are lower than those of CSQG and EU for all samples and higher than the average upper earth crust values of Wedepohl. These metals were released to the environment from both natural and anthropogenic sources; however, releases from anthropogenic sources are greater than those from natural sources, while

Table 2 Reference range of heavy metals of the soil (mg/kg).

Samples	Fe	Zn	Cu	Pb	Cd	Reference
Grade I[a]		100	35	35	200	SEPA (1995)
Grade II[b]		300	100	350	1000	SEPA (1995)
Average shale	47,200	95	45	20	0.3	Turekian and Wedepohl (1961)
CSQG (Agriculture soil)	–	200	63	70	1.4	CCME (2007)
European Union Standards	–	300	140	300	3	EU (2002)
Average upper earth crust	30,890	14.3	52	17	0.1	Wedepohl

[a] The natural background level in soils of China (SEPA, 1995).
[b] The value for protecting agricultural production and human health (SEPA, 1995).

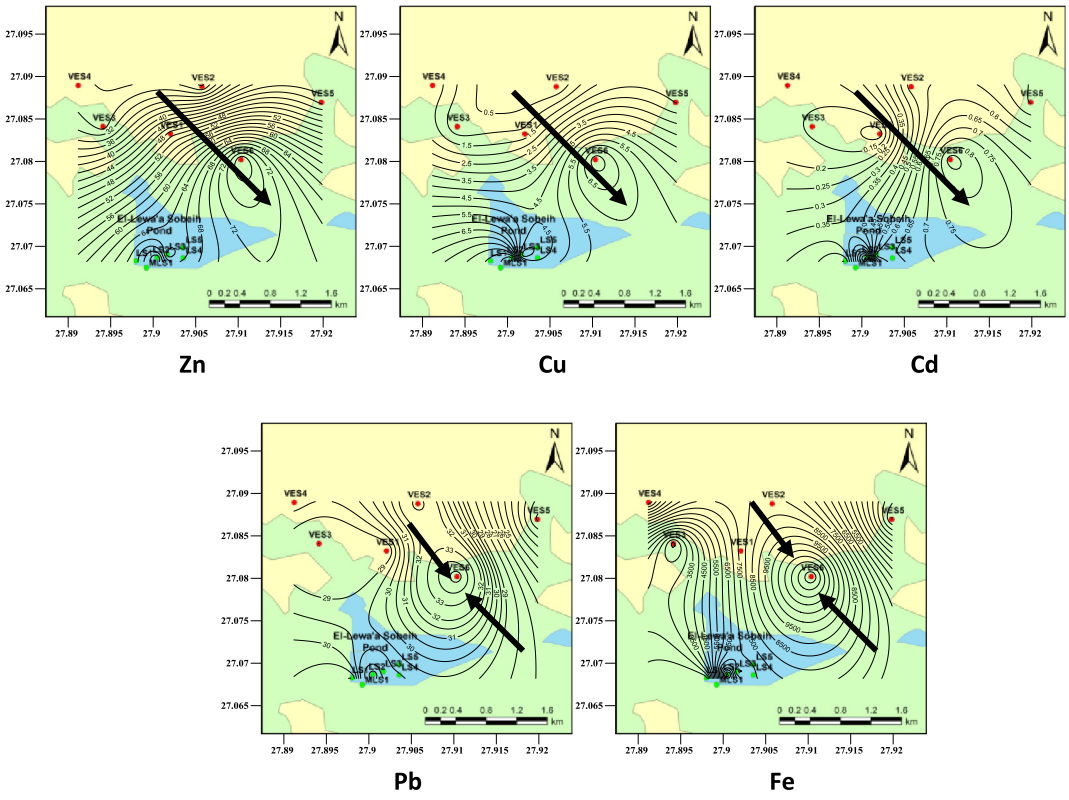

Figure 9 Heavy metal distribution.

Cu concentrations in the study area are lower than both values of CSQG, EU and the average upper earth crust of Wedepohl.

Zn, Cu and Cd decrease toward the northwestern direction, while Pb and Fe increase toward the location of VES 6 (Fig. 9).

3. Results and conclusions

The superficial geoelectrical layer is mainly composed of shale (Dakhla Shale Formation). It is characterized by low resistivity values (3–5 Ω m). The depth of this layer ranges from 2.56 to 17.58 m.

The second layer is composed of saturated sandstone sediments saturated with wastewater infiltrated from the oxidation pond with moderate electrical resistivity values (17–98 Ω m). This layer was extended to the end of the investigated section.

Grain size analysis revealed that all samples are sand (94.5–99.6%) and rarely mud (0.4–0.5%) with exception at VES 6 where the mud is the dominant. The sand increases toward the northern direction. In general, the mud% and mean% decrease toward the northern direction away from El-Lewa'a Sobeih pond with inverse trend with sand% which increases toward the northern direction. The percentage of total organic carbon, total carbonate percentage and total phosphorous is decreased toward the northern direction. Zn, Cu and Cd decrease toward the northwestern direction, while Pb and Fe increase toward of VES 6.

The most promising area for cultivation locates along the two electrical profiles at the area under investigation where located thick thickness of shale formation.

The most geochemical analysis for soil samples indicates that there is some pollution in the soil due to seepage from the oxidation pond.

The eastern and western part of the area under investigation exhibits a thicker shale layer. So, these parts are proper

for site reclamation and agriculture activities depending on the treated sewage water without side effect on the shallow groundwater.

References

Abbas, M.A., Sultan, S.A., 2008. 2-D and 3-D resistivity in the area of the Menkaure Pyramid Giza, Egypt. Bull. Eng. Geol. Environ. 67, 411–414.

Aspila, K.I., Agemian, H., Chau, A.S.Y., 1976. A semi-automated method for the determination of inorganic, organic and total phosphate in sediments. Analyst 101, 187–197.

Balba, A.M., 1985. Fifty years of phosphorus studies in Egypt. Adv. Soil Water Res. (5), 118, spec vol..

Beadnell, H.J.L., 1901. Farafra Oasis, its topography and geology. Geol. Surv. Egypt, Cairo. 39p.

Bodek, I., Lyman, W.J., Reehl, W.F., Rosenblatt, D.H., 1988. Environmental inorganic chemistry: properties, processes, and estimation methods. In: Walton, B.T., Conway, R.A. (Eds.), SETAC Special Publication Series. Pergamon Press, New York.

Canadian Soil Quality Guidelines (CSQG), 2007. Canadian soil quality guidelines (CSQG) for the protection of environmental and human health: Summary tables. Updated September, 2007. In: Canadian environmental quality guidelines, 1999, Canadian Council of Ministers of the Environment, Winnipeg by Canadian Council of Ministers of the Environment (CCME).

El-Sayed, H.M., 2010. Environmental investigation on Lake Maryut, west of Alexandria, Egypt: geochemical, geophysical and remote sensing studies M.Sc. Thesis. Alexandria University, Egypt.

European Union, 2002. Heavy Metals in Wastes, European Commission on Environment. <http://ec.europa.eu/environment/waste/studies/pdf/ heavymetalsreport.pdf> (Eutrophication and nutrient release in urban areas of sub-Saharan Africa – a review. Sci. Total Environ. 408, 447–455).

Folk, R.L., 1980. Petrology of Sedimentary Rocks. Hemphill Publishing Company, Austin, Texas, p. 182.

Gosh, D.A., 1971. The application of geoelectrical resistivity measurements. Geophys. Prospect. 19, 192–217.

Hemeker, C.J., 1984. Vertical Electrical Sounding Model Interpretation Program. IWCO, The Netherlands.

Hermina, M., 1990. The surroundings of Kharga, Dakhla and Farafra oases. In: Said, R. (Ed.), The Geology of Egypt. Egyptian General Petroleum Corporation, pp. 259–292.

Issawi, B., Francis, M., Youssef, A., Osman, R., 2009. The Phanerozoic of Egypt: A Geodynamic Approach. Geological Survey of Egypt, Cairo, p. 589.

Koefoed, O., 1965a. A generalized Cagniard graph for the interpretation of geoelectrical sounding data. Geophys. Prospect. 8, 459–469.

Koefoed, O., 1965b. A semi direct method of interpreting resistivity observations. Geophys. Prospect. 13 (2), 259–282.

Koefoed, O., 1965c. A direct methods of interpreting resistivity observations. Geophys. Prospect. 13 (4), 568–591.

Loring, D.H., Rantala, R.T.T., 1992. Manual for the geochemical analysis of marine sediments and suspended particulate matter. Earth Sci. Rev. 32, 255–285.

Mohamaden, Mahmoud.I.I., 2001. Evaluation of the quaternary aquifer between qena and luxur (Nile Valley, Egypt). Qatar Univ. Sci. J. 21, 75–95.

Mohamaden, M.I.I., Shagar, S. Abu, 2008. Structural effect on the groundwater at the Arish City, North eastern Part of Sinai Peninsula, Egypt. Egypt. J. Aquat. Res. 35 (2), 31–47.

Mohamaden, M.I.I., 2008. Groundwater exploration at Rafah, Sinai Peninsula, Egypt. Egypt. J. Aquat. Res. 35 (2), 49–68.

Mohamaden, M.I.I., Abu Shagar, S., Abdallah, Gamal A., 2009. Geoelectrical survey for groundwater exploration at the Asyut Governorates, Nile Valley, Egypt. J. King Abdulaziz Univ. Mar. Sci. 20, 91–108.

Mohamaden, M.I.I., 2005. Electric resistivity investigation at Nuweiba Harbour of Aqaba, South Sinai, Egypt. Egypt. J. Aquat. Res. 31 (1), 58–68.

Molnia, B.F., 1974. A rapid and accurate method for the analysis of calcium carbonate in small samples. J. Sed. Petrol. 44 (2), 589–590.

Murphy, J., Riley, J.P., 1962. A modified single solution method for the determination of phosphate in natural waters. Anal. Chim. Acta 26, 31–36.

Omara, S., Hemida, I., Sanad, S., 1970. Structure and hydrogeology of Farafra Oasis, Western Desert, UAR. In: 7th Arab Petroleum Congress, Kuwait, paper 65.

Orabi, O.H., Zaky, A.S., 2016. Differential dissolution susceptibility of Paleocene foraminiferal assemblage from Farafra Oasis, Egypt. J. Afr. Earth Sc. 113, 181–193.

Oregioni, B., Aston, S.R., 1984. The determination of selected trace metals in marine sediments by flame atomic absorption spectrophotometry IAEA Monaco Lab. Int. Rep.

Said, R., 1962. The Geology of Egypt. Elsevier, Amsterdam, p. 377.

Santos, F.A.M., Sultan, S.A., Represas, P., El Sorady, A.L., 2006. Joint inversion of gravity and geoelectrical data for groundwater and structural investigation: application to the northwestern part of Sinai, Egypt. Geophys. J. Int. 165, 705–718.

SEPA, State Environmental Protection Administration of China, 1995. Environmental quality standard for soils, GB15618-1995.

Sultan, S.A., Santos, F.A.M., 2008. Evaluating subsurface structures and stratigraphic units using 2D electrical and magnetic data at the area north Greater Cairo, Egypt. Int. J. Appl. Earth Obs. Geoinf. 10, 56–67.

Sultan, S.A., Santos, F.A.M., Helaly, A.S., 2009. Integrated geophysical interpretation for the area located at the eastern part of Ismailia Canal, Greater Cairo, Egypt. Saudi Society for Geosciences.

Sultan, A.S., Santos, F.M., 2009. Combining TEM/resistivity joint inversion and magnetic data for groundwater exploration: application to the northeastern part of Greater Cairo, Egypt. Environ. Geol. 58, 521–529.

Sultan, A.S., Mohameden, M.I.I., Santos, F.M., 2009. Hydrogeophysical study of the El Qaa Plain, Sinai, Egypt. Bull. Eng. Geol. Environ. 68, 525–537.

Turekian, K.K., Wedepohl, K.H., 1961. Distribution of the elements in some major units of the Earth's crust. Geol. Soc. Am. Bull. 72 (2), 175e192.

Zohdy, A.A.R., 1975. Automatic interpretation of Schlumberger sounding curves using modified Dar Zarrouk functions. Bull. 13 B-E. U.S. Geological Survey.

Zohdy, A.A.R., 1989. A new method for the automatic interpretation of Schlumberger and Wenner sounding curve. Geophysics 54 (2), 245–253.